QUASI-AUTOMATIC GEOMETRIC CORRECTION AND RELATED GEOMETRIC ISSUES IN THE EXPLOITATION OF CHRIS/PROBA DATA

Luis Alonso, Jose Moreno

Laboratory for Earth Observation, Universidad de Valencia (Spain), Email: luis.alonso@uv.es

ABSTRACT

The multiangular and off-track pointing capabilities of CHRIS/PROBA introduce a strong distortion on the geometry on the resulting images.

In order to make full scientific use of the data some information about the geometry of acquisition is needed. In particular, the viewing azimuth and zenith angles must be known, and the images must be geometrically corrected to make possible multi-angular and multi-temporal studies.

CHRIS/PROBA images are distributed with ancillary data related to its acquisition. The angles provided with the images, Minimum Zenith Angle (MZA) and Fly-by Zenith Angle (FZA), accurately determine the satellite-target geometry, but they are not the ones needed for atmospheric / angular corrections, and the information provided with the data is not enough to derive the required geometric information.

There is an urgent need of precise methods to obtain the CHRIS/PROBA data in a practical format. That means precise Azimuth and Zenith Observation Angles for each image, and accurate geometric correction of the images. Also, the great volume of images provided demands, in order to be practical, that these methods should be automatic with a minimum intervention for quality checks in the processing.

1. INTRODUCTION

Before scientific use of satellite images they need some preprocessing (e.g. geometric and atmospheric correction) to convert them to the physical values of interest for each study.

The objective for CHRIS is to provide Earth surface hyperspectral reflectance data with a wide range of different viewing configurations, and provide Bidirectional Reflectance Distribution Function (BRDF), for atmospheric, land and coastal studies [1].

Geometric correction transforms images, as they are acquired by the sensors, to match a certain cartographic projection, free of distortions; and each pixel is assigned with coordinates. Several methods exist to perform geometric correction, each one with pros and cons.

Atmospheric correction removes effects of the atmosphere on the radiation from the surface that arrives to the sensor; it also converts the physical values of the image from radiance to ground reflectance. But it needs accurate observation and illumination angles for each pixel.

Other scientific studies also need observation and illumination angles; some examples are research of angular effects, retrieval of biophysical parameters from surface BRDF, or surface albedo determination.

1.1 Geometric Correction

After receiving the first CHRIS/PROBA image set we performed a ground control point (GCP) correction over a georeferenced Landsat image, to quickly produce geometrically corrected images. But this method is time consuming and the interpolation applied cannot correct all the distortions in an image, especially in areas where there are few features to set as GPC. This method becomes unpractical for coastal waters, and inapplicable for open sea scenes.

Each CHRIS/PROBA acquisition is a set of up to five images taken with different view angles [2]. Geometric correction must be applied independently to each image. In the case of extreme observations (FZA=+-55) GCP are very difficult to determine with precision, what introduces further distortions in the geometric correction using this method. GCP correction is very time consuming, and becomes unpractical for processing of a time series of acquisitions.

Also the correction of images with different view angles introduces a problem of resampling. Due to the different viewing geometry the pixel size is variable, but after coregistration they must have the same size, therefore interpolation is required. But standard methods are not always satisfactory.

At present the general method to correct CHRIS/PROBA images is using Ground Control Points [1]. More sophisticated alternatives are available: e.g. co-registration method, but they present other problems, as interpolation, or the lack of providing observation angles.

1.2 Knowledge of Observation Angles

The determination of the solar illumination angles can be easily obtained knowing the geographical coordinates of the target and the time of the acquisition. But the observation angles of each pixel cannot be obtained by direct methods without previous knowledge about the sensor design and operation, and the satellite position and orientation at acquisition time.

Proc. of the 2nd CHRIS/Proba Workshop, ESA/ESRIN, Frascati, Italy
28-30 April (ESA SP-578, July 2004)

The angles provided with the images, Minimum Zenith Angle (MZA) and Fly-by Zenith Angle (FZA), accurately determine the mean satellite-target geometry [3]. But their definitions are based on engineering criteria and are very useful to operate the satellite, but they are not appropriate for scientific analysis. Therefore it is necessary to convert MZA and FZA to standard view azimuth and zenith angles.

PROBA is capable to manoeuvre pointing off-track to acquire images of sites even when the satellite does not pass directly above them.

In order to operate PROBA needs to know where to point to, that is, what rotations it has to perform so the programmed target falls within the field of view of CHRIS sensor. These rotations are more easily defined with respect to the position in the orbit of maximum approach to the target. At this moment the satellite is flying over a certain location that we designate sub-satellite position at maximum approach (SSMA), and the view zenith angle to the target is minimum for this orbit (MZA). The SSMA serves as reference point to define the Fly-by Zenith Angle (FZA). These angles are univocally related to the observation azimuth and zenith angles, as reflected in Fig. 1.

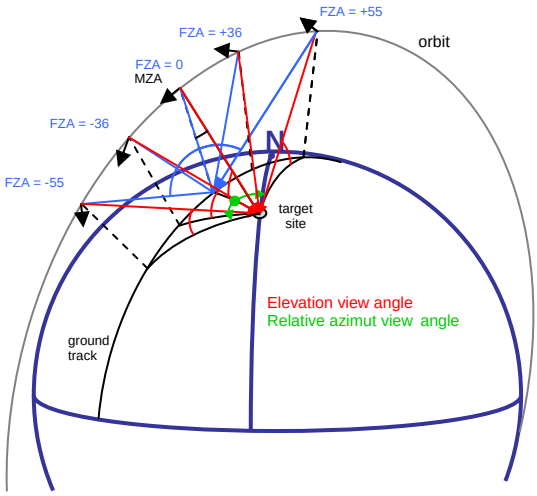

Fig. 1. Relationship between engineering and observation view angles

1.3 Parametric Method

A quasi-automatic parametric method (a mathematical orbit/attitude model) is desired, because it reproduces the acquisition process; thus it does not require GCPs except a few in order to correct for small deviations from nominal actuation of the satellite. It also provides accurate observation angles, and actual pixel sizes, allowing the use of better interpolation methods that take into account the point spread function (PSF) of the sensor.

The problem is that the ancillary data available with the images provided are not enough to apply parametric correction directly.

2. DETERMINATION OF OBSERVATION ANGLES

Scientific applications require the knowledge of observation angles. In order to calculate view azimuth and zenith angles from the MZA and FZA there are various possible approaches:

- Orbit propagation from TLEs
- Spherical geometry calculations
- As by-product of parametrical geometric correction.

The first, based on orbital mechanics, is more rigorous but its application is complex.

The second is based on geometrical relationships and makes some approximations. It is simple and fast.

The last provides an accurate calculation of the view angles, but it is currently under development, so we are using only the first two.

2.1 Orbit Propagation

The orbital elements of a satellite are a set of parameters that determine the orbit that the satellite is following at a given moment. Using these orbital elements with the appropriate orbital model it is possible to calculate the position and velocity in space of the satellite at any given time past or future; this is called orbit propagation. The model allows calculating the viewing angles of the satellite from a given point in the surface of the earth, among other parameters.

The CHRIS/PROBA team makes available the orbital elements for the satellite in a daily basis in the form of Two Line Elements (TLE) calculated by the EE.UU. NORAD surveillance system [4]. These TLEs must be used with the NORAD's SGP4/SDP4 orbital model [5]. In particular we have used the TrackStar implementation of the orbital model developed by T. S. Kelso.

In case of very stable orbits the propagation from a given set of orbital elements can be very accurate for long periods of time. In the case of PROBA its orbit is low and suffers of atmospheric drag and other types of perturbations, because of that it is very unstable and the propagations are only accurate within a few weeks. Therefore, to calculate the observation angles of a given image set it is recommended to use the closest TLE available.

To calculate the observation angles from the known MZA and FZA the model must be run setting the observation point at target location (TGT), to determine the time of maximum approach (i.e. the moment when

MZA is reached), and the corresponding sub-satellite coordinates (SSMA).

Then, it is run again using the SSMA coordinates as target to get the times when Fly-by Zenith Angle (FZA) ±55 and ±36 occur. Finally, going back to the first run to obtain the observation angles at the proper time stamps.

The whole process is schematized in Fig. 2 as flow chart.

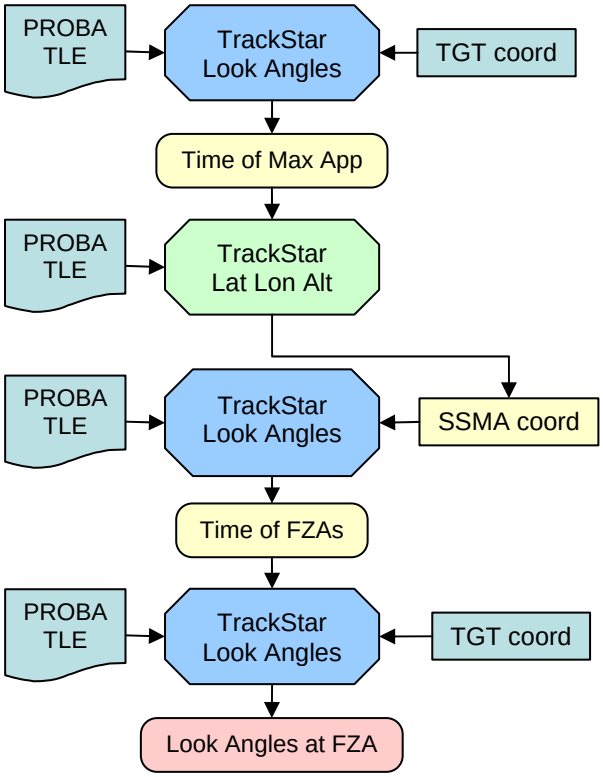

Fig. 2 Flow chart for determination of view angles by orbital propagation.

This method is not practical because it requires several runs and the available models need code rewriting in order to automate the process; so simpler ones are needed.

2.2 Spherical Geometry

Due to the need of a simple method to know the actual view angles we have obtained the relationship between the engineering angles (FZA, MZA) and the observation zenith angles, by means of spherical geometry. At present the assumptions are spherical Earth and circular orbit, but the precision obtained is sufficient.

$$A = FZA - asin(Rt/(Rt+H)*sin(FZA))$$

$$B = MZA - asin(Rt/(Rt+H)*sin(MZA))$$

$$C = acos(cos(A)*cos(B))$$

$$\mathbf{VZ} = c + atan(sin(C), (Rt+H)/Rt - cos(C))$$

$$\mathbf{RVA} = asin(sin(A)/sin(C))$$

Where ***Rt*** is mean Earth radius, ***H*** is the altitude of the satellite, ***VZ*** is the view zenith angle, and ***RVA*** is the relative azimuth angle. The fuction atan(x,y) returns the angle whose tangent is equal to x/y in the [-π,π] range.

Azimuth observation angles obtained in this way are relative to the maximum approach direction, so a second relationship is found between the MZA and the inclination of the orbit to determine the actual Observation Azimuth Angle.

The MZA defines a circle of radius ***R*** around the target. The inclination ***i*** of the orbit limits the possible ground tracks to two solutions. The sign of the MZA determines which one of the two is the correct solution, as illustrated in Fig. 3.

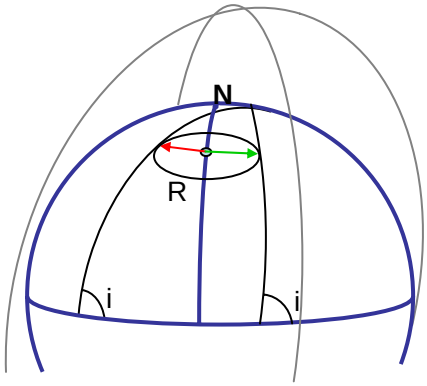

Fig. 3. Determination of the actual view azimuth angle.

2.3 Comparison of Results

To test these two simpler methods we used the images corresponding to the SPARC campaign, which took place in Barrax (Spain) between the 12th and the 14th of July 2003. There were images available the first and last days, unfortunately the acquisition of the 13th (nadir view pass) failed.

We used the following data with the spherical geometry approach and the orbit propagation model.

The coordinates of the site:

39.047N, -2.073E 700m ASL

The TLE from the 12th of July:

```
1 26958U 01049B   03193.84088317  .00001065
00000-0  11503-3 0   243
2 26958  97.8423 271.3000 0083543 329.7739
29.8652 14.88062739 93418
```

The provided MZA in the HDF files were:

MZA = 20º on the 12th of July
MZA = -27º on the 14th of July

The inclination of the orbit is 97.8423º (from the TLE).

Both methods provide similar results with the greatest difference being azimuth at maximum approach (the

fastest varying parameter), and it is less than 1 degree. Results are summarized in Fig. 4 and Tables 1 and 2.

Table 1. Calculated view angles for the image set of SPARC campaign using spherical geometry.

FZA	+55	+36	0	-36	-55
12/07/2003					
Azimuth	26.11	37.98	102.40	165.44	177.06
Zenith	55.99	38.78	19.40	39.15	56.24
14/07/2003					
Azimuth	353.77	339.44	285.27	231.22	216.91
Zenith	57.29	42.44	27.60	42.53	57.40

Table 2. Calculated view angles by orbital propagation

12/07/2003 Orbital Propagation method					
Azimuth	26.093	37.654	101.568	165.412	176.946
Zenith	56.025	39.132	19.420	39.146	56.042

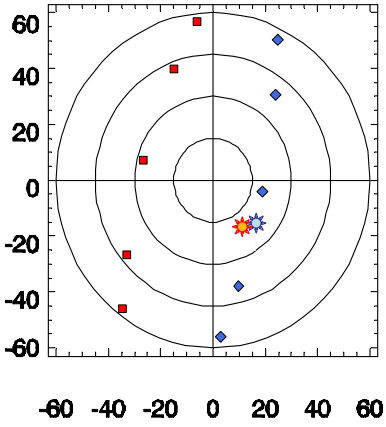

Fig. 4. Polar plot, showing the angular configuration for the SPARC campaign. Data corresponding to the 12th of July in blue diamonds, 14th of July in red squares.

2.4 Side Effects of Slow-down Factor

The previous methods provide easy solutions that do not need much effort to implement. They make some assumptions, that in general are appropriate, but there is one that can be problematic: the consideration that during the acquisition of an image the observation conditions do not change substantially.

In reality, the satellite uses the forward motion to perform the scanning process, and at the same time rotates slightly to keep the target pointed for a longer time in order to increase the signal to noise ratio [6]. This means that the distance covered by the satellite is longer than the surface scanned, and the effect is as if the satellite was travelling slower. The ratio between both distances is known as slow-down factor.

Due to the slow-down factor applied to increase integration time, the angles of observation of the first and last lines of the image are no longer equal. This difference is larger for larger slow-down factors. In the case of CHRIS/PROBA, its slow-down factor of 5 introduces noticeable variation in the observation angles throughout the image.

So the solutions provided by the simpler algorithms represent only the mean value of the observation angles. For most applications this is sufficient, but for some others, especially BRDF and angular effects studies, more precise values are necessary.

Fig. 5 illustrates how the slowdown factor increases the angles of observation within one image acquisition. It also shows that the scanning direction is reversed at ±36º from the forward advance of the satellite. This is designed so in order to reduce the rotation rate needed to operate the satellite.

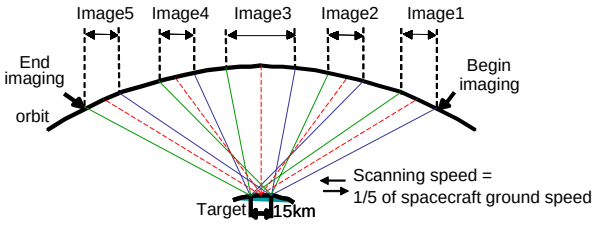

Fig. 5. Scheme of the actual acquisition procedure of CHRIS/PROBA with slowdown factor.

We have calculated what would be the actual range of view angles within every image of the SPARC campaign, which includes large off-track pointing (MZA=-27) and almost nadir pointing (MZA=-4). We also calculated it for a theoretical case of nadir passing. The results are shown in Tables 3 and 4 and depicted in Fig. 6.

To calculate these ranges we have used the orbital propagation model, and we needed to make some assumptions as close to the real case as possible: The time that takes to acquire any image is always 10s and the acquisition begins 5s before reaching FZA (dashed red line in Fig. 5). Also we have considered, for simplicity, that the sensor is always pointing to the centre of the scene; this implies that we disregard the reverse scanning for FZA=±36, so our results in these cases would be slightly underestimated.

Table 3. Range of view angles at start, mid and end of image acquisition for close to nadir observation.

FZA	MZA=-4	Time	Azimuth	Zenith
+55	start:	11:18:11	9.5788	56.3865
	mean:	11:18:16	9.4395	55.0605
	end:	11:18:21	9.2864	53.6715
			Δ=0.2924	Δ=2.7150
+36	start:	11:19:04	6.9338	38.3996
	mean:	11:19:09	6.4430	36.1887
	end:	11:19:14	5.8681	33.8844
			Δ=1.0657	**Δ =4.5152**
0	start:	11:20:06	316.8270	5.8263
	mean:	11:20:11	282.9885	4.8691
	end:	11:20:16	249.4303	5.8694
			Δ=67.3904	Δ =1.0003
-36	start:	11:21:07	201.2887	32.8952
	mean:	11:21:12	200.6692	35.2457
	end:	11:21:17	200.1428	37.5028
			Δ=1.1459	**Δ =4.6076**
-55	start:	11:22:02	197.5760	53.6986
	mean:	11:22:07	197.4198	55.0929
	end:	11:22:12	197.2780	56.4188
			Δ=0.2980	Δ =2.7202

Table 4. Range of view angles at start, mid and end of image acquisition for extreme off-nadir observation.

FZA	MZA=-27	Time	Azimuth	Zenith
+55	start:	11:30:28	354.5574	58.426
	mean:	11:30:33	353.7555	57.2739
	end:	11:30:38	352.894	56.0837
			Δ=1.6634	Δ=2.3423
+36	start:	11:31:21	341.3062	43.8842
	mean:	11:31:26	339.2435	42.2938
	end:	11:31:31	336.9521	40.6844
			Δ=4.3541	**Δ=3.1998**
0	start:	11:32.24	291.5198	27.7363
	mean:	11:32:29	285.2442	27.5978
	end:	11:32:34	278.9715	27.7503
			Δ=12.5483	Δ=0.1525
-36	start:	11:33:27	233.7256	40.7545
	mean:	11:33:32	231.438	42.3671
	end:	11:33:37	229.3746	43.9636
			Δ=4.351	**Δ=3.2091**
-55	start:	11:34:21	217.6533	56.3717
	mean:	11:34:25	216.965	57.3247
	end:	11:34:31	216.0072	58.7031
			Δ=1.6461	Δ=2.3314

If we look at the results, we see that the difference of angles at start and end of the image of the azimuth and zenith angles are very different depending on the FZA and MZA. For FZA=0 the effect is stronger in azimuth; even for a pass very close to nadir (MZA=-4) the zenith angle has only a variation of ~1º, but when it reaches MZA=0 the zenith angle has the greatest variation ~6.5º, and the azimuth angle has only a change in the direction (180º). At FZA=±36 the change affects both azimuth and zenith angles, and with exception of the nadir case, it has the greatest zenith variations. In the cases of FZA=±55 the variation is smaller and affects more the zenith angle.

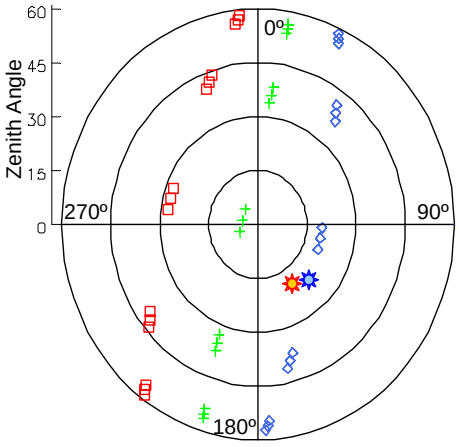

Fig. 6. Polar representation of the calculated observation angles at start, mid and end of each image acquisition.

In order to represent with a single magnitude the range of the observation angles we have considered the azimuth and zenith angles as coordinates of a unitary vector in spherical coordinates. Then we have calculated the scalar product of the start and end vectors, which is related to the angle formed by both vectors.

The resulting quantities, in Table 4, show that the absolute angle variation within the images is similar at each FZA independent of the MZA, being more important in the case of maximum approach (FZA=0). But the contribution of azimuth and zenith angles to this variation depends on how far is the overpass from nadir, as described previously.

Table 5. Absolute angle variation due to slowdown factor in SPARC images and a theoretical nadir case.

	+55	**+36**	**0**	**-36**	**-55**
MZA =-27	2.73	4.34	5.83	4.35	2.71
MZA = 20	2.63	4.48	6.17	4.48	2.75
MZA = -4	2.73	4.56	6.48	4.65	2.73
MZA = 0	2.76	4.58	6.51	4.58	2.76

3. SIMPLE GEOMETRIC CORRECTION

A simple geometric correction is possible by using the zenith and azimuth viewing angles together with basic orbital information and making the assumption of instantaneous image acquisition. The image is then

projected onto the surface of the Earth using the across-track Field of View (FOV) and an effective along-track Field of View.

Because the sensor is "push-broom" type there is not a real FOV, just an Instant Field of View for each line, so an effective FOV for the whole scene must be used that can be estimated taking into account the duration of the acquisition, a reference pointing profile and the slow-down factor.

This method could be adequate for those orbits which overfly the target very close to nadir, and always using some GCP to adjust the correction. In the case of off-track pointing this approach might not very reliable.

We do not expect the method to be accurate enough to provide a satisfactory result by itself, but it is automatic and gives a better starting point for the application of GCP correction, reducing drastically the number of control points required (i.e. less time required) and improving results.

4. PARAMETRIC GEOMETRIC CORRECTION

A parametric correction method would be able to describe rigorously the acquisition process [7], and to provide accurate results needed for scientific purposes.

The idea is to reconstruct the position and orientation of the sensor at each instant of the acquisition process making possible to determine the actual geographical coordinates of each pixel. To do the orbit reconstruction it is necessary to combine all the available data from PROBA (TLE and telemetry data).

Taking into account that the acquisition of a single image takes 10s and it has 748 lines, this means that the time precision needed is 1/100 of a second in order to have the time reference assigned to a single line. Such precision is required to link GCP and orbital parameters that help to increase accuracy in the correction process.

Telemetry data available in the image headers is by far too coarse to be useful for a parametric approach to geometric correction, although some parameters (e.g. calculated image centre time) could be useful together with the corresponding TLE if no other telemetry data is available.

Fortunately the full telemetry data received at the PROBA control ground station has a time precision of 1/1000 of second , that greatly satisfies the precision required; but it is updated every 25s which is longer than the acquisition time of a single image [8]. The orbit is quite stable within that lapse of time, so interpolation is a satisfactory solution. In the case of attitude, the pointing manoeuvre takes place in a matter of few seconds, therefore the telemetry data is not enough precise for direct correction procedure, and an estimation of the attitude is necessary.

After orbit determination, one can reconstruct the attitude reference profiles in the satellite reference in the same way as the satellite computes the Guidance Profile Generation [9]. Since the method does not require the derivatives of such angles (the satellite needs the second derivative to compute forces) the computation is rather straightforward, and then a simple algorithm allows geolocation.

Initially all error is attributed to the fact that initial attitude data used by the satellite to compute the guidance profile can be slightly wrong due to the filtering of star-tracker data [1], and then GCPs are used to recompute the reference initial attitude for the same attitude guidance profile. If this is not enough the residuals can then be used to model polynomials in time for the deviations in attitude angles during the acquisition sequence (a second-degree polynomial in time during each one of the five acquisitions). We want to combine all these corrections with a very sophisticate resampling technique [10] to compensate the different ground spatial resolutions for each angular view, something possible if a detailed reconstruction of the observation geometry is available.

A general scheme of the whole process is synthesized in Fig. 7, where the dependencies between the different steps are reflected, and the role of GCPs as mean of error reduction.

Despite its complexity, this method is very convenient, in particular when a large amount of images must be processed. In the case of open coastal waters, where the number of available GCPs is small or even inexistent, this method becomes the only reasonable solution to corregistration of images.

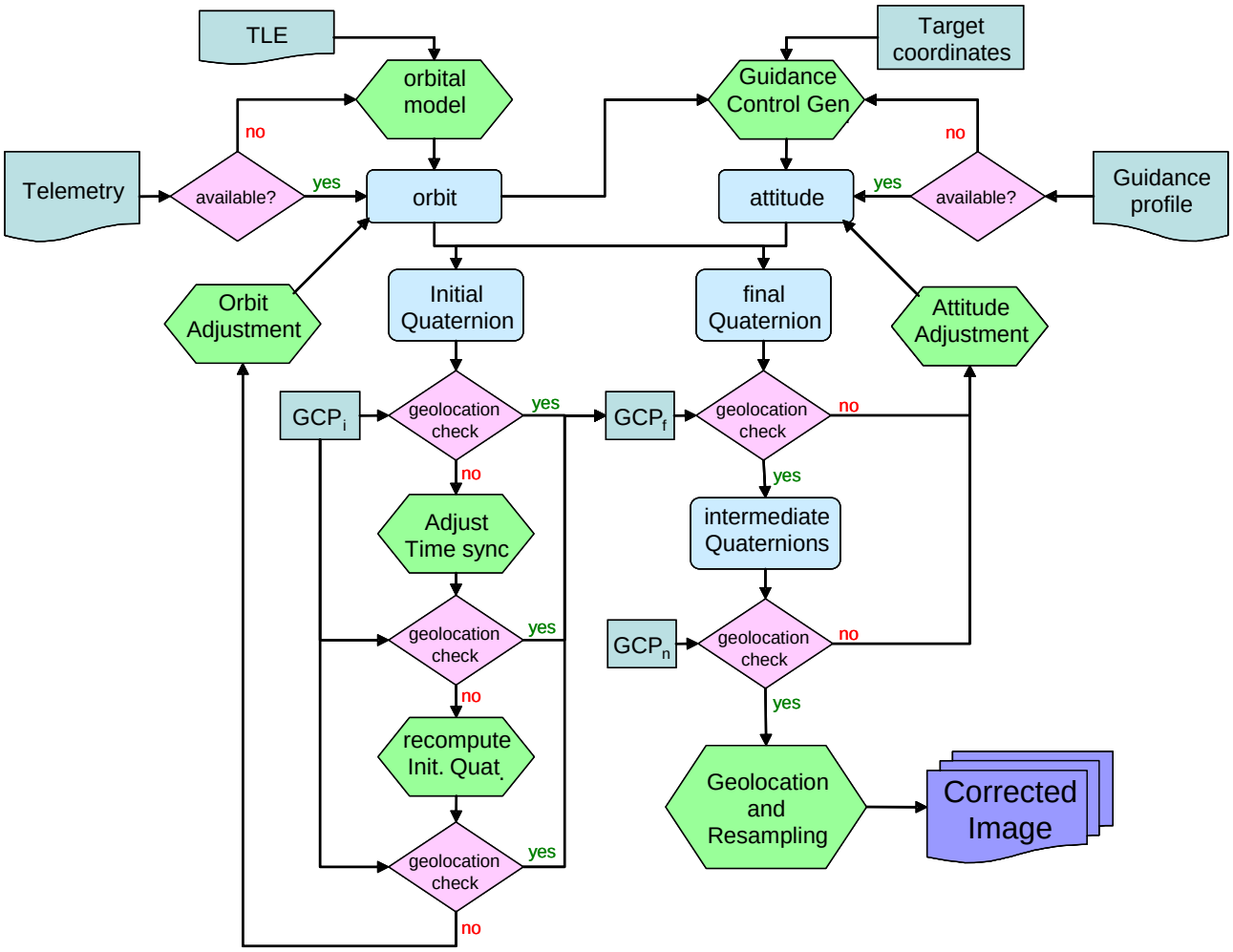

Fig. 7. Flow chart of the parametric algorithm for geometric correction.

5. CONCLUSIONS

In the present work we analyse the problems related to the geometry of a complex dataset as it is the multi angular image set from CHRIS/PROBA, namely:

- The calculation of the observation angles of each single image: the angles (MZA and FZA) provided with the images are related to the operation of the satellite, and only indirectly to the observation angles.

- The effect of the slowdown factor: due to the acquisition manoeuvres to increase the radiometric performance of the sensor, the view angles are not constant within each image. For precise BRDF studies the actual view angles should be calculated.

We propose a general method for the geometric correction of CHRIS/PROBA images based on the physical modelling of orbit and attitude parameters and such method will also provide accurate observation angles for every single pixel. This method provides almost automatic correction of the images, with the use of just a few GCP needed to assess the accuracy of the telemetry and attitude.

Some advantages of the proposed method are

- it can operate with minimum supervision, so it can handle large number or images in short time.

- it can work without GCPs (at the cost of accuracy) allowing the georectification of open water images.

- it provides accurate observation angles in per-pixel basis

- it solves the problem of resampling pixels of different sizes

Until full development of this geometric correction procedure, more simplistic approaches have been presented for immediate use:

- Spherical geometry relationships to obtain view angles from data available in the image header.

- An orbital propagation method that uses published TLE data, with similar results to the spherical geometry solution.

- A “photographic model” that could help to accelerate the geometric correction process by standard GCP procedure.

It is certain that many users are facing similar problems related to the geometric correction procedure, but it is also sure that most users cannot (or do not want) to enter into this kind of technical details.

The same is true for removal of noises, atmospheric corrections, etc. but it seems that the geometrical problem is particularly crude, and the current situation where users have even difficulties to compute elementary magnitudes such as view zenith and azimuth angles should be corrected. Some generic procedure, operational but accurate enough, would be quite useful for the CHRIS/PROBA community.

ACKNOWLEDGEMENT

This work has been supported by the ESA project SPARC RFQ/3-10824/03/NL/FF. We would like to thank the kind help of Mike Cutter and Jeff Settle.

REFERENCES

1. ESTEC, *Exploitation of CHRIS data from the PROBA mission for science and applications*, http://www.estec.esa.nl/proba/doc/proba_handbook.pdf ESA Scientic Campaign Unit, ESTEC 1999, Noordwijk, The Netherlands.

2. Barnsley M.J., Settle J.J., Cutter M., Lobb D. and Teston F., The PROBA/CHRIS mission: a low-cost smallsat for hyperspectral, multi-angle, observations of the Earth surface and atmosphere, *IEEE Transactions on Geoscience and Remote Sensing*, Accepted for print, 2004

3. Cutter M. A., *CHRIS Data Format*, SIRA Electro-Optics 2002, London, U.K.

4. Kelso T. S., *Description of NORAD Two-Line Element Set Format*, http://www.celestrak.com/NORAD/documentation/tle-fmt.shtml

5. Hoots R. L., Roehrich R. L., Kelso T. S., *Spacetrack Report Number 3 Models for Propagation of NORAD Elements Sets*, http://www.celestrak.com/NORAD/documentation/spacetrk.pdf

6. Van den Braembussche P., de Lafontaine J., Vuilleumier P., PROBA Attitude Control and Guidance In-orbit Performance, *Proceedings of the 5th Intl. ESA Conference on Spacecraft Guidance, Navigation and Control Systems*, Fracati, Italy, 22-25 October 2002, (ESA SP-516, Feb 2003)

7. Moreno J., Meliá J., A method for accurate geometric correction of NOAA AVHRR HRPT data, *IEEE Transactions on Geoscience and Remote Sensing*, Vol. 31, 204-226, 1993

8. Montenbruck O., Vuilleumier P., In-flight Performance Analysis of the PROBA Onboard Navigation System, DLR/GSOC, June 2003, Germany.

9. de Lafontaine J., Buijs J., Vuilleumier P., Van der Braembussche P., Development of the PROBA Attitude Control and Navigation Software, *Proceedings of the 4th Intl. ESA Conference on Spacecraft Guidance, Navigation and Control Systems*,ESTEC, Noordwijk, The Netherlands, 18-21 October 1999, (ESA SP-425, Feb 2000)

10. Moreno J., Meliá J., An optimum interpolation method applied to the resampling of NOAA AVHRR data, , *IEEE Transactions on Geoscience and Remote Sensing*, Vol. 32, 131-151, 1994